Validation of OSCAR Surface Currents in the Western Arctic Marginal Seas against Saildrone Observations

Nan-Hsun Chi[1], Dongxiao Zhang[12], Chidong Zhang[1]

[1] NOAA Pacific Marine Environmental Laboratory, Seattle, WA 98115

[2] The Cooperative Institute for Climate, Ocean and Ecosystem Studies, University of Washington, Seattle, WA 98105

Key Points:

- This study validates OSCAR satellite derived surface currents in the western Arctic, including the very shallow waters, by saildrones.
- High vector correlation but larger vector difference between OSCAR and saildrone currents often occur in strong topography guided currents.
- Low vector correlation occurs at weaker currents, over the shallow Hanna Shoal, and near fresher waters due to ice melt and river discharge.

Key Words:

Surface currents, saildrone, OSCAR, western Arctic marginal seas, validation against in situ observation

Abstract:

The western Arctic marginal seas undergo large seasonal variation, but are very challenging to observe directly due to sea ice and shallow depths. Deployments of several saildrone uncrewed surface vehicles (USVs) in the summers of 2018 and 2019 provided unique opportunities to

validate the satellite-derived near surface currents, Ocean Surface Current Analysis Real-time (OSCAR), in the western Arctic marginal seas against in situ upper ocean current measurements. Overall, OSCAR current is biased low with significant noise. Higher vector correlation and speed difference often occur where stronger currents (often topography-steered) are observed. Such differences reveal that the dataset resolvability depends on spatial and temporal resolutions, smoothing, and latitudes, suggesting that OSCAR is able to depict the major current systems but significantly underestimates their strength. Poorer vector correlation occurs at weaker current regimes (< 10 cm/s), over the shallow Hanna Shoal, near fresher water due to ice melt and river discharge. The latter two water class regimes highlight the importance of salinity contribution to the buoyancy force which is neglected in the OSCAR formulation.

Plain Language Summary:

It is challenging to make direct measurements in the western Arctic marginal seas, which undergo large seasonal swings, because of the sea ice and shallow depths. We validate the satellite-derived surface current product, Ocean Surface Current Analysis Real-time (OSCAR), against observations from saildrone uncrewed surface vehicles (USVs) in the western Arctic marginal seas cruising in summers of 2018 and 2019. Overall, OSCAR current is biased low and noisy. Higher current direction relation and speed differences often occur where stronger currents are observed. Such differences suggest that the reliability of OSCAR depends on several factors. It also suggests that OSCAR is able to depict the major current systems but significantly underestimates their strength. Poorer current direction relation occurs at weaker current regimes, over the shallow Hanna Shoal, near fresher water due to ice melt and river discharge. The latter two regimes highlight the importance of salinity information, which however, is neglected in the OSCAR model.

1. Introduction

The near surface currents in the western Arctic marginal seas (i.e., the Bering, Chukchi, and Beaufort Seas) play important roles in various geophysical phenomena, such as the transport of heat, salt (e.g., Woodgate et al., 2018, Woodgate and Peralta-Ferriz, 2021), and sea ice (Krumpen et al., 2019, DeRepentigny et al., 2020). Monitoring the surface current variation is therefore essential for studying the fate of the Pacific-origin waters into the Arctic basin and its impact on the Arctic ecosystem (Stabeno, 2019).

Accurate knowledge of the upper surface currents systems in the western Arctic marginal seas is important in estimating the transport and fluxes of various physical properties and matters. The state-of-art global near surface ocean currents products (i.e., OSCAR) are not directly measured by satellites but derived from the satellite measurements using simplified formulation (Bonjean and Lagerloef, 2002). As the sea surface height measurements in the high latitudes become available after 2010s from emergence of new satellite products and now being used (i.e., Cryosat-2) in the latest OSCAR near surface current products, these large-scale near surface current estimates are extended to polar oceans. On the other hand, satellite observations show declining Arctic sea ice extent for all months (Serreze and Stroeve, 2015, Stabeno and Bell, 2019), shortened ice season (Wang et al., 2018) and related to the greater rising of surface temperatures than the global mean surface temperature (Serreze and Francis, 2006, Richter-Menge et al., 2019). Climate forecast models also suggest that in the Arctic the surface air temperature will continue to rise much faster and the summertime sea-ice extent will continue to decline (Alexander et al., 2018, Jefferies et al., 2013). Therefore, the spatial extent and the length of direct air-sea interaction in the ice-free part of the Arctic, which could be measured from the satellites, is increasing and may eventually become normal during summer in a warmer climate.

Validating the high latitude satellite-derived near surface products against in situ measurements is therefore important in advancing the understanding of aforementioned geophysical phenomena towards higher latitudes oceans, including the western Arctic marginal seas.

The western Arctic marginal seas feature many shallow shelf regions and mobile sea ice which not only prevent Argo float measurements but also limit research ships from complete surveys, therefore very challenging for in situ observations. Saildrone uncrewed surface vehicles (USVs) provide a unique opportunity to measure air-sea interaction over the very shallow waters on the shelf and ice edge in western Arctic marginal seas. Saildrones are wind and solar powered vehicles that allow deployments lasting up to 12 months and provide high quality, near real-time, multivariate upper ocean and atmospheric observations (Zhang et al. 2019). The primary goal of this work is using the saildrone arrays to validate the satellite-derived ocean surface current products, OSCAR, in the western Arctic marginal seas. Our analysis should be taken as a preliminary step in the comparison of large scale gridded upper ocean current data to encourage future research and application in this region.

In this study we focus on subsurface current velocities measured by current profilers described in section 2.1. These saildrone provide valuable and rare in situ current observation in the seasonal ice zone or gaps of ship observations. These observations are instrumental in advancing our knowledge for further development and verification of satellite observation, satellite-derived data products, and numerical models. Recent studies used two saildrones to validate various satellite SST products and SMAP SSS products in the western Arctic (Vazquez-Cuervo et al., 2021, Vazquez-Cuervo et al., 2022). As the satellite-based products evolve constantly with emergence of new satellites and frequent changes of algorithms for improving their absolute accuracy, it is vital to do periodic validation against in situ data. Among eight of

L4 satellite SST products, NOAA/NCEI DOISST and the RSS MWOI SST are shown to have better relative accuracy against saildrone. Also, the SMAP SSS products are shown to resolve the runoff signal associated with the Yukon River discharge with high correlation between SMAP products and saildrone 0.5 m salinity. Both MWOI SST and SMAP SSS products from Remote Sensing System (RSS) described in 2.3 are therefore chosen to be used in this study.

The manuscript is organized as follows. Section 2 describes the data and methods. Section 3 presents the results. Section 4 summarizes this paper.

2. Data and Methods

2.1 In-Situ Saildrone Data

In situ data used in this study are from two saildrones deployed in July - September of 2018 (1020, 1021) and three saildrones (1035, 1036, 1037) deployed in May - September 2019 (Chiodi et al., 2021). They were launched from Dutch Harbor, Alaska crossed the Bering Strait into the Chukchi Sea (and Beaufort Sea in 2019) and headed south for recovery as the sunlight hours became short (Figure 1,2).

The surface current is measured by the downward looking 300 kHz Workhorse WHM300-I-UG1 acoustic Doppler current profilers (ADCP) mounted on the keels of the five saildrones. The vertical resolution of the ADCP data is 2 m. The temporal resolution of the 5-miniute average ADCP currents analyzed here are on 1020, 1021, 1035, and 10 minutes on 1036, 1037, on which ADCPs were turned on and off for 5 minutes every 10 minutes to save power.

The saildrone ADCP data is often easier to process than those of the ship-board ADCP. The saildrone's transiting speed is slow – on average speed of 0.96 m/s, or ~18% of the average wind speed at 5.4 m/s during the 2019 deployment (Chiodi et al., 2021). This quiet vehicle is less affected by bubble issues (Joseph, 2014). The ADCP data is generally reliable ~5 m below the

sea surface. Depending on the echo intensity, ADCP data typically extend to 60-100 m depth, ideal for survey of the entire water column on the shelf. The saildrone ADCP has onboard motion correction for preliminary quality control before the data are sent to the data center in near real time. However, additional steps, including removing data below the ocean floor, or where echo intensity is too small, or where the vertical velocity is too large, are necessary to remove unrealistic current estimates and to achieve an accuracy of 2-3 cm/s.

The near surface temperature and salinity were measured at a nominal depth of 0.5 m by 2 saildrones in summer 2018 and 3 saildrones in summer 2019. The unpumped RBR sensors were available in both years and the pumped SBE sensors were available in 2019. Here we use RBR measurements in 2018 and SBE measurements in 2019. The RBR data are available every 10 minute on 1020, 1021 and the SBE data are available every 5 minute on 1035, 1036, 1037. The temperature and salinity data analyzed are 1-miniute averages of 1-Hz measurements. Simple QC are applied to the temperature and salinity data by removing those with large 1-minute standard deviation (0.1 degC for temperature and 0.05 psu for salinity).

2.2 OSCAR Data

OSCAR (Ocean Surface Current Analysis Real-time) is a global near-surface (nominal depth at 15 m) ocean current product derived from sea surface height, ocean surface vector winds and sea surface temperature observed by various satellites and in situ instruments. The model formulation combines geostrophic, Ekman and thermal wind dynamics (e.g., the local acceleration and non-linearities are not represented. Bonjean and Lagerloef, 2002). Its version 2.0, on ¼ degree with a 1-day resolution, is used in this study.

The OSCAR calibration and validation (https://www.esr.org/research/oscar/validation/) using both 15 m drogued drifters and moorings suggest that its known problem areas fall in 3

main categories: eddy-dead regions such as the Alaskan Gyre, the meridional component around the equator and near coasts. Smoothing in creation of the regular gridded source data and during the calculation of spatial gradients would consistently underestimate the speeds compared to those of drifters, generally by 50-60% globally. Parts of the western Arctic marginal seas could fall in the last case where the model is not accurate very close to coastlines or ice, since source satellite signals can be corrupted there.

2.3 Satellite Sea Surface Temperature and Salinity Data

Sea surface temperature (SST) and sea surface salinity (SSS) data are both from Remote Sensing Systems (RSS) (Meissner et al., 2022). The SST product is the RSS Microwave (MW) OI SST version 5.1 (daily mean). The SSS data is SMAP version 5.0 Level 3 8-day running mean by RSS on 1-day nominal resolution. Both SST and SSS products are distributed in a 0.25˚ rectangular projection. This latest SMAP RSS version uses a new sea ice flag and sea ice correction including detection of large drifting icebergs.

2.4 Satellite Ancillary Data – AVISO FES 2014 Tide Database

AVISO FES 2014 tides database is used to remove the barotropic tidal current from the in situ saildrone measured current. FES2014 was produced by Noveltis, Legos and CLS and distributed by Aviso+, with support from Cnes (https://www.aviso.altimetry.fr/). It is a global tide solution that uses finite element mesh, T-UGO barotropic model and data assimilation of altimetry and tidal gauges.

Removing tidal currents are necessary in order to compare with OSCAR, the non-tidal near surface currents products. Previous studies have documented the regional-dependent characteristics of tides along the western Arctic marginal seas (i.e., Foreman et al., 2006, Huang et al., 2011, Mofjeld et al., 1986). The northeastern Chukchi Sea appears to be non-tidal and is

often dominated by currents driven by synoptic weather patterns. Tidal currents are also weak in the eastern Chukchi shelf (amplitude < O(5 cm/s)). In the Bering Sea tidal current amplitudes are significant (on O(40 cm/s)) especially near coastlines of the Bristol Bay, Kuskokwim Bay and Norton Sound.

2.5 Collocation and Statistical Evaluation of OSCAR

We use nearest-neighbor interpolation to first match each saildrone measurements (5-minute or 10-minute) with the OSCAR gridded data in time and space. For each unique gridded OSCAR data point, all saildrone data are averaged within that grid cell for a single match-up saildrone data point. Figure 3 shows the time series of the collocated saildrone 10-20 m layer averaged current vectors in 2019 around the OSCAR grids and their vector differences.

The evaluation of the differences between OSCAR and saildrone current speed are quantified objectively by several statistical metrics including bias, root-mean-square error (RMSE), standard deviation of the errors (SDE), and signal-to-noise ratio (SNR). The definitions of the statistical metrics follow Vazquez-Cuervo et al. (2022). The vector correlation is the cosine similarity as the cosine of the angle between the collocated OSCAR and saildrone current vectors.

3. Results

Figure 1ab shows 3 saildrone tracks during summer 2019. They were deployed from Dutch Harbor in mid-May and made their way off Alaska's west and northwestern coastline through the Bering Sea and up through Bering Strait around June 5th 2019. Then the saildrone stayed in the Chukchi Sea shelf until July 2019 and reached the farthest northern latitude ~75.5 N in the Beaufort Sea in August before returning to Dutch Harbor in early October. The near surface waters are remarkably colder and fresher in the Beaufort Sea than those on the Bering

and Chukchi shelves (Figure 1ab, 2). The saildrones also measured the very warm and fresh surface waters, associated with seasonal warming and freshening, west of Yukon-Kuskokwim delta (Y-K delta) in early June 2019 (Vazquez-Cuervo et al., 2021, 2022). The surface waters on the shelf are significantly warmed in 3 months of the saildrone deployment (Figure 1,2); the Bering Sea shelf is freshened especially near the Alaskan coast.

The saildrones in summer 2018 went similar routes in the Bering Sea and Chukchi Sea from July to the end of September but did not reach the Beaufort Sea. The fresh and warm signals associated with Yukon River discharge are not as obvious as in July 2019. The difference is consistent with the climatology of the seasonal variation west of the Y-K delta (Figure 9 of Vazquez-Cuervo et al., 2022), with SSS dipping seasonally around mid-May to mid-June and increasing afterwards, and SST increasing seasonally from April to July.

3.1 Overall Comparison between Saildrone and OSCAR datasets

Figure 4 summarizes the overall data distribution in direction bins of every 22.5^{o} and several specific subsets of the collocated saildrone 10-20 m layer averaged and OSCAR 15 m current data, the current speed difference and vector correlation between the two current datasets. The spokes represent the direction of which current vectors are towards. Colors along the spokes indicate the parameters specified (i.e., speed, speed difference, or vector correlation). The length of each spoke and its colored segment represents the percentage occurrence of the currents (as numbered) flowing towards a particular direction at a given parameter range. Their overall speed difference is notable (Figure 4abc), with OSCAR currents weaker than saildrones by 5.3 cm/s (Table 1). Underestimation can be due to smoothing and spatial resolution of satellite data in creating the regular-grid OSCAR products. 67% of the collocated velocity pairs are fairly correlated (with direction difference within 67.5^{o}), and is consistent between using 2018 current

data only (67%) and 2019 only (70%). The slope of the linear regression line indicates that OSCAR in general underestimates the current speeds and their zonal or meridional velocities by 50-100% (Figure 5). The RMSD, which characterizes the variability in the difference of the two datasets, is 11 cm/s. The SDE, in which the mean bias (5.3 cm/s) was removed, is 9.6 cm/s. RMSD and SDE are both more profound than the mean bias, and on the same order of magnitude as the observed SD, suggesting notable speed difference from observation. The signal-to-noise ratio (SNR), which is inversely proportional to SDE, is 0.8. In fact, the SNR of all subsets is smaller than 1, indicating that the noise of OSCAR current speed overwhelms the real signals.

3.2 Comparisons between Saildrone and OSCAR datasets in different current speed regimes

The strong current regime (current speed > 30 cm/s) is observed mostly in bathymetry guided flows, i.e., in the Bering Strait where currents flow northward in early June 2019, upstream Barrow Canyon where currents flow eastward in July 2019, and on the Chukchi Slope where Chukchi Slope Currents flow northwestward in the end of July 2019 (Figure 1,3). Their vector correlation is well above average (64% of vector correlation is > 0.92, i.e., less than 22.5-degree deviation from each other). The negative bias and RMSD of the OSCAR current speed are of the same order of magnitude (O(20 cm/s) and significantly larger than average (Figure 4efg, Table 1). This phenomenon is consistent with the lower-than-1 linear regression slope and small intercept (Figure 5a). The SDE is half of the RMSE and larger than the observed SD, indicating the differences in current speed of the strong current regime is significant and considerably contributed by underestimation.

For the weak current regime (current speed < 10 cm/s), the overall vector correlation is lower than average, more than ⅖ is either orthogonal or negatively correlated. In contrast,

OSCAR current speed is positively biased by 0.8 cm/s, also indicated by the positive intercept of y-axis in Figure 5a. The RMSD and SDE are twice the observed SD. It suggests that for the weaker current regime the OSCAR current speed is significantly different from observation and with slight overestimation.

3.3 Comparisons between Saildrone and OSCAR datasets in different water classes or areas

The collocated OSCAR and saildrone currents show poorer vector correlation than average at the cold fresh water lenses from ice melting and warm fresh Yukon River discharge (Figure 4pt, Table 1). The RMSD and SDE of current speed for both water classes are slightly larger than the observed SD, indicating significant current speed difference. The SNR is reduced to half compared to the overall statistics, indicating the OSCAR current speeds in these two surface water classes are excessively overwhelmed by noise. These lighter surface water lenses from ice melting or river outflow that increase the near surface stratification are commonly present in summertime. However, the buoyancy force is only a function of SST but not SSS in OSCAR formulation (Bonjean and Lagerloef, 2002). Since salinity dominates the density variation in the cold-water regime, it suggests that the salinity contribution to the buoyancy gradient to the Ekman current velocities could be significant. Large stratification near the surface could also induce large shear near the surface, which could potentially modulate the ocean response to the winds, and their air-sea momentum transfer.

On the other hand, there are areas with very shallow bathymetry on the Chukchi Sea shelf near the west Alaskan coast where the saildrones had chances to make measurements in 2018 and 2019. The vector correlation at the shallow bathymetry on the eastern Chukchi shelf is similar to the overall statistics (Table 1). The vector correlation is poorer around Hanna Shoal

where the bathymetry is also shallow and current speed is slightly weaker. The RMSD and SDE of both subsets are slightly larger than the observed SD, and with reduced SNR compared to the overall statistics. Similar to the aforementioned two water classes, the OSCAR current speeds in the shallow water are of significant difference from observation and excessively overwhelmed by noise. Larger uncertainties near the coastlines, within 100 km, are known problems in the OSCAR model (section 2.2).

4. Summary

This work presents rare upper ocean current measurements from saildrone USVs in the Bering Sea shelf, Chukchi Sea shelf and slope regions, and Beaufort Sea, where shallow depths prevent most research vessels from completing surveys. We use saildrone in situ data from the summers of 2018 and 2019 to validate the OSCAR satellite derived current products. This work quantifies the uncertainty of the OSCAR near surface currents and highlights the regimes to expect larger negative biases of current speed or lower vector correlation. The overall current speed difference for the collocated OSCAR and saildrones is significant (SDE larger than the observed SD), with OSCAR under-estimating the observed speed. Particularly, the OSCAR satellite derived currents data in the western Arctic is 50-100% lower than the observations. For comparison, globally the derived currents data is 50-60% lower than in situ data observed from 15 m drogued drifters and moorings from the global network of OceanSITES. Such differences reveal that the dataset resolvability depends on spatial and temporal resolution, smoothing, and latitudes. In addition, the signal-to-ratio (SNR) of the OSCAR current speeds is lower than 1 in western Arctic marginal seas, indicating an overwhelming noise level in the dataset.

Higher vector correlation occurs at the strong current regime where currents are guided by the bathymetry. The negative speed bias of the strong current regime is O(20 cm/s). This

implies that OSCAR is able to depict the major current systems in the western Arctic marginal seas but significantly underestimates their strength. Low vector correlation is often observed for weaker currents, for example, in the Hanna Shoal area, or in stratified surface waters from either the warm fresh river discharge or the cold fresh surface melt waters. The SNR of OSCAR is also significantly reduced in the Hanna Shoal area and the aforementioned lighter surface waters. The poor statistical results for the two water classes highlight the importance of the salinity information especially in cold water regimes for the vertical momentum diffusion, though neglected in the OSCAR model.

This analysis serves as a preliminary step toward comparing and validating large scale gridded upper ocean current products to encourage future research and application in the western Arctic and other parts of the world's oceans using saildrone data. In particular, repeated saildrone missions in some key areas in the western Arctic marginal seas would be beneficial in monitoring and quantification of the Pacific water inflow rates and routes. On the other hand, saildrones can be used to validate and improve the satellite-derived surface current data in high latitude oceans so that not only the Pacific water surface routes but in the other parts of high latitude surface water routes and properties can be better estimated under the warming climate.

Acknowledgments:

This is PMEL Contribution #5406.

Open Research:

The NASA saildrone data is accessed from https://podaac-tools.jpl.nasa.gov/drive/files/allData/insitu and the NOAA saildrone data is from

https://data.pmel.noaa.gov/pmel/erddap/info/index.html?page=1&itemsPerPage=1000. ESR; Dohan, Kathleen. 2021. Ocean Surface Current Analyses Real-time (OSCAR) Surface Currents - Final 0.25 Degree (Version 2.0). Ver. 2.0. PO.DAAC, CA, USA. Dataset accessed pm 2022-06-01 at https://doi.org/10.5067/OSCAR-25F20. Meissner, T., F. J. Microwave OI SST data are produced by Remote Sensing Systems and sponsored by National Oceanographic Partnership Program (NOPP) and the NASA Earth Science Physical Oceanography Program. Data is available at www.remss.com. SMAP salinity data are produced by Remote Sensing Systems and sponsored by the NASA Ocean Salinity Science Team. Data are available at www.remss.com. FES2014 was produced by Noveltis, Legos and CLS and distributed by Aviso+, with support from Cnes (https://www.aviso.altimetry.fr/).

References:

Alexander, M.A., Scott, J.D., Friedland, K.D., Mills, K.E., Nye, J.A., Pershing, A.J., Thomas, A.C. (2018), Projected sea surface temperatures over the 21st century: Changes in the mean, variability and extremes for large marine ecosystem regions of Northern Oceans. Elementa: Science of the Anthropocene, 6 9. https://doi.org/10.1525/elementa.191

Joseph, A. (2014), Chapter 11 - Vertical Profiling of Currents Using Acoustic Doppler Current Profilers. Measuring Ocean Currents, Elsevier, 339-379, ISBN 9780124159907, https://doi.org/10.1016/B978-0-12-415990-7.00011-9

Bonjean, F., & Lagerloef G.S.E. (2002), Diagnostic model and analysis of the surface currents in the tropical Pacific Ocean. J. Phys. Oceanogr., vol. 32, pg. 2938-2954, https://doi.org/10.1175/1520-0485(2002)032<2938:DMAAOT>2.0.CO;2

Boury, S., Pickart, R. S., Odier, P., Lin, P., Li, M., Fine, E. C., et al. (2020), Whither the Chukchi Slope Current?, *Journal of Physical Oceanography*, *50*(6), 1717-1732, https://journals.ametsoc.org/view/journals/phoc/50/6/JPO-D-19-0273.1.xml

Chiodi, A.M., Zhang, C., Cokelet, E.D., Yang, Q., Mordy, C.W., et al. (2021), Exploring the Pacific Arctic Seasonal Ice Zone with Saildrone USVs. Front. Mar. Sci. 8:640690. https://doi.org/10.3389/fmars.2021.640697

Corlett, W. B., & Pickart, R. S. (2017), The Chukchi slope current, Progress in Oceanography, Volume 153, Pages 50-65, ISSN 0079-6611, https://doi.org/10.1016/j.pocean.2017.04.005

Foreman, M.G.G, Cummins, P.F., Cherniawsky, J.Y. and Stabeno, P. (2006), Tidal Energy in the Bering Sea. J. Mar. Res., 64:797-818, https://doi.org/10.1357/002224006779698341

Huang, L., Wolcott, D., & Yang, H. (2011), Tidal characteristics along the Western and Northern coasts of Alaska. In US Hydro 2011 Conference, Florida, https://legacy.iho.int/mtg_docs/rhc/ArHC/ArHC3/ARHC3-3.2.4_TidalCharacteristicsAK.pdf

Jeffries, M.O., Overland, J.E. & Perovich, D.K. (2013), The Arctic shifts to a new normal. Physics Today 66:35–40, https://doi.org/10.1063/PT.3.2147

Krumpen, T., Belter, H.J., Boetius, A., Damm, E., Haas, C., Hendricks, S., et al. (2019), Arctic warming interrupts the Transpolar Drift and affects long-range transport of sea ice and ice-rafted matter. Scientific Reports, 9(5459), 1–9, https://doi.org/10.1038/s41598-019-41456-y

Meissner, T., F. J. Wentz, A. Manaster, R. Lindsley, M. Brewer, M. Densberger, (2022), Remote Sensing Systems SMAP Ocean Surface Salinities [Level 3 Running 8- day], Version 5.0 validated release. Remote Sensing Systems, Santa Rosa, CA, USA. Available online at www.remss.com/missions/smap, doi: 10.5067/SMP50-3SPCS

Mofjeld, H. O. (1986), Observed tides on the northeastern Bering Sea shelf, J. Geophys. Res., 91(C2), 2593– 2606, https://doi.org/10.1029/JC091iC02p02593

Richter-Menge, J., Osborne, E., Druckenmiller, M., and Jeffries, M.O. (2019), The Arctic, in ["State of the Climate in 2018"]. Bull. Am. Meteorol. Soc. 100 (9), S141-145, https://doi.org/10.1175/2019BAMSStateoftheClimate.1

Stabeno, P., Kachel, N., Ladd, C., Woodgate, R. (2018), Flow patterns in the eastern Chukchi Sea: 2010–2015. Journal of Geophysical Research: Oceans, 123, 1177–1195, https://doi.org/10.1002/2017JC013135

Stabeno, P. J. (2019), The Eastern Bering Sea: declining ice, warming seas, and a changing ecosystem [in "State of the Climate in 2018"]. Bull. Am. Meteorol. Soc. 100, S148–S149, https://doi.org/10.1175/2019BAMSStateoftheClimate.1

Stabeno, P.J., & Bell, S.W. (2019), Extreme conditions in the Bering Sea (2017-2018): record breaking low sea-ice extent. Geophys. Res. Lett. 46, 8952–8959, https://doi.org/10.1029/2019GL083816

Serreze, M.C., & Stroeve, J. (2015) Arctic sea ice trends, variability and implications for seasonal ice forecasting. Phil. Trans. R. Soc. A 373: 20140159, http://dx.doi.org/10.1098/rsta.2014.0159

Vazquez-Cuervo, J., Gentemann, C., Tang, W., Carroll, D., Zhang, H., Menemenlis, D., et al. (2021), Using Saildrones to Validate Arctic Sea-Surface Salinity from the SMAP Satellite and from Ocean Models. Remote Sens, 13, 831, https://doi.org/10.3390/rs13050831

Vazquez-Cuervo, J., Castro, S.L., Steele, M., Gentemann, C., Gomez-Valdes, J., Tang,W. (2022), Comparison of GHRSST SST Analysis in the Arctic Ocean and Alaskan Coastal Waters Using Saildrones. Remote Sens. 14, 692, https://doi.org/10.3390/rs14030692

Walsh, J.J., McRoy, C.P., Coachman, L.K., Goering, J.J., Nihoul, J.J., Whitledge, T.E., et al. (1989), Carbon and nitrogen cycling within the Bering/Chukchi Seas: Source regions for organic matter effecting AOU demands of the Arctic Ocean, Progress in Oceanography, Volume 22, Issue 4, Pages 277-359, ISSN 0079-6611, https://doi.org/10.1016/0079-6611(89)90006-2

Woodgate, R.A., Stafford, K.M., Prahl, F.G. (2015), A synthesis of year-round interdisciplinary mooring measurements in the Bering Strait (1990-2014) and the RUSALCA years (2004-2011), Oceanography 28(3):46-67, https://doi.org/10.5670/oceanog.2015.57

Woodgate, R.A. (2018), Increases in the Pacific inflow to the Arctic from 1990 to 2015, and insights into seasonal trends and driving mechanisms from year-round Bering Strait mooring data, Progress in Oceanography, 160, 124-154, https://doi.org/10.1016/j.pocean.2017.12.007

Woodgate, R. A., & Peralta-Ferriz, C. (2021), Warming and freshening of the Pacific inflow to the Arctic from 1990-2019 implying dramatic shoaling in Pacific Winter Water ventilation of the Arctic water column. Geophy. Res. Letters, 48, e2021GL092528, https://doi.org/10.1029/2021GL092528

Zhang, D., M.F. Cronin, C. Meinig, J.T. Farrar, R. Jenkins, D. Peacock, J. Keene, A. Sutton, and Q. Yang. (2019), Comparing air-sea flux measurements from a new unmanned surface vehicle and proven platforms during the SPURS-2 field campaign. *Oceanography* 32(2):122–133, https://doi.org/10.5670/oceanog.2019.220

Table 1: Summary of statistical differences between the collocated OSCAR and saildrone current speed and vector correlation under several specific subsets described in the leftmost column with the number of pairs in the parenthesis. Obs. SD is the observed current speed by saildrones. RMSD is root-mean-square-difference. Bias is the mean residual difference, OSCAR-SD. SDE is the standard deviation of errors in which the mean bias error is removed. SNR is the signal-to-noise ratio. R is the vector correlation coefficient described in Figure 4. R> 0.38, |R|< 0.38, and R< -0.38 refers to the angle between collocated vectors smaller than 67.5°, between 67.5° and 112.5°, and between 112.5° and 180° respectively.

	Obs. SD (cm/s)	Bias (cm/s)	RMSD (cm/s)	SDE (cm/s)	SNR (cm/s)	Percentage of current vector correlation (%)		
						R>0.38	|R|<0.38	R<-0.38
Overall (2267)	11.5	-5.3	11.0	9.6	0.80	67	14	17
Current > 30 cm/s (237)	10.3	-20.6	24.2	12.8	0.80	88	5	7
Current < 10 cm/s (896)	2.4	0.8	4.8	4.8	0.92	56	19	25
Cold fresh T< 2C, S< 27psu (127 from 2019)	7.1	-3.2	8.0	7.3	0.38	43	24	32
Yukon River Discharge T> 5C, S< 28psu (12 from 2019)	4.2	-4.8	7.2	5.4	0.40	58	33	8
Hanna Shoal > -30m (44)	4.9	-4.8	7.1	5.3	0.60	55	14	32
> -30m (96)	8.7	-6.0	10.9	9.0	0.46	67	13	20

Figure 1: Three saildrone tracks (1035, 1036, 1037) in 2019 colored by (a) saildrone 0.5 m salinity and (b) saildrone 0.5 m temperature. Two saildrones (1020, 1021) in 2018 colored by (c) saildrone 0.5 salinity and (d) saildrone 0.5 m temperature. The contour background is the bathymetry. The thin black contours are depth contours of -50, -200 and -1000 m. The magenta texts are the dates (mm/dd) of the locations of 1036 in 2019 and of 1020 in 2018.

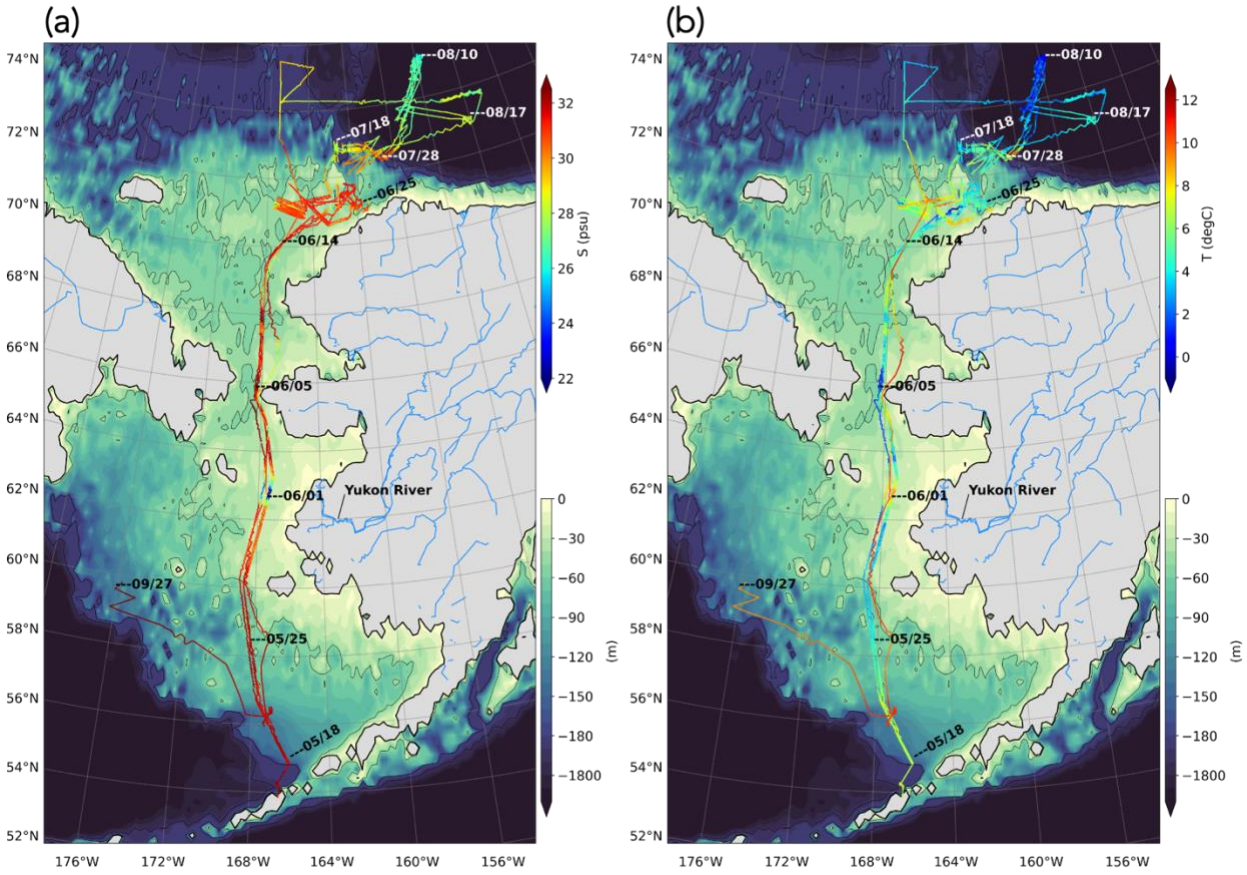

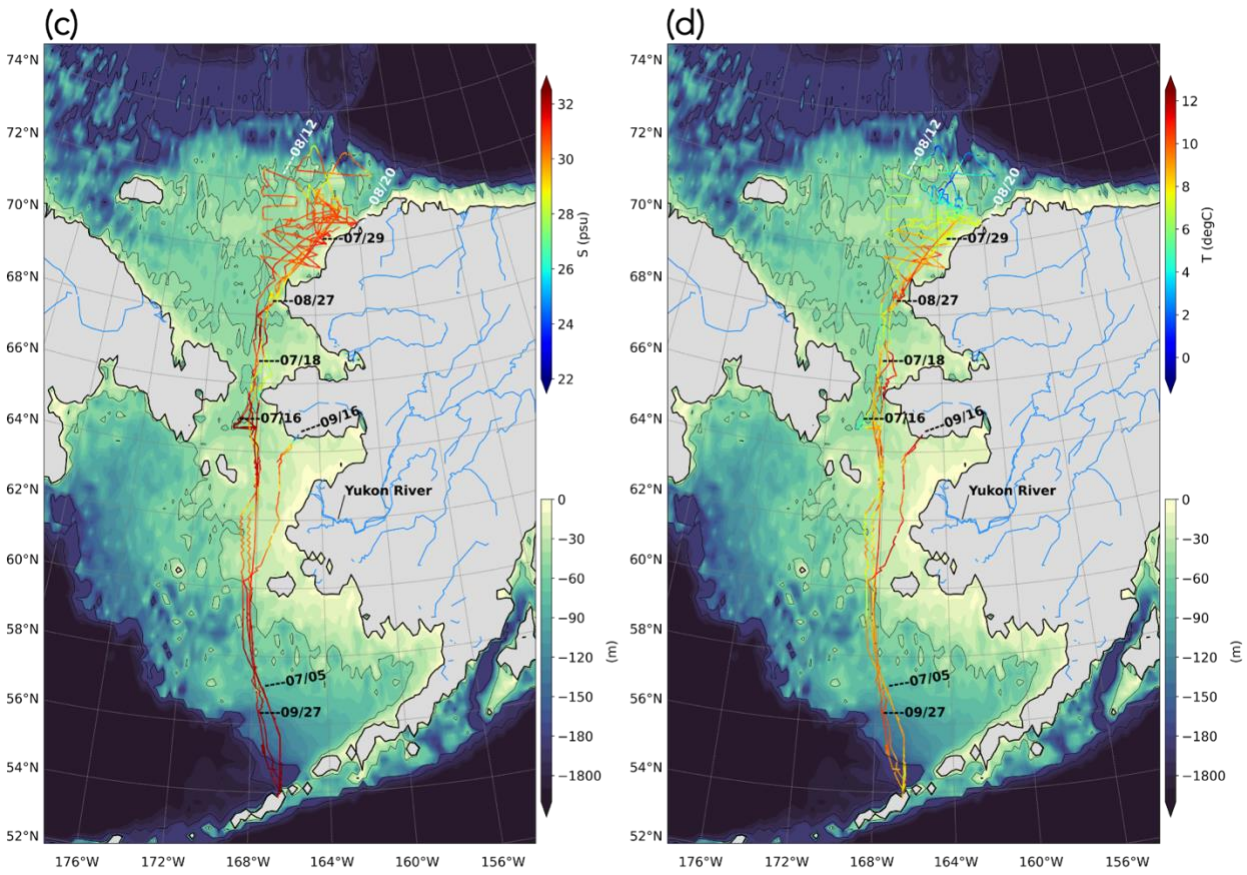
(c)
(d)
74°N
72°N
70°N
68°N
66°N
64°N
62°N
60°N
58°N
56°N
54°N
52°N
176°W
172°W
168°W
164°W
160°W
156°W
08/12
08/20
07/29
08/27
07/18
07/16
09/16
07/05
09/27
Yukon River
S (psu)
T (degC)
(m)

427
428

Figure 2: Satellite maps of (a,c) SSS and (b,d) SST on (a,b) 2019/05/15 and (c,d) 2019/09/15. The bathymetry contour levels are the same as in Figure 1. Data with sea ice concentration larger than 0.1, or uncertainties larger than 1 psu for SSS and 1 ºC for SST are not plotted.

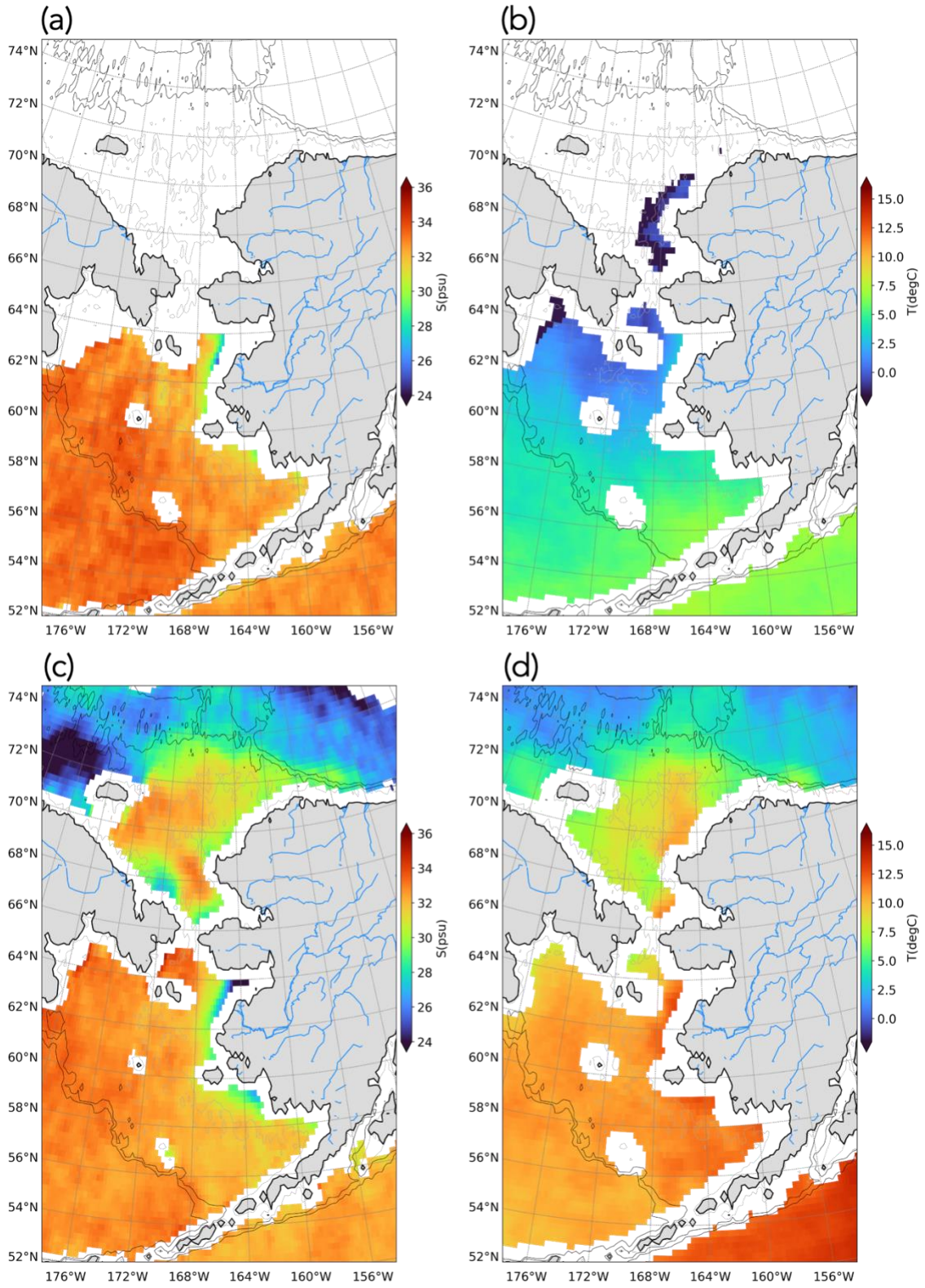

Figure 3: The time series of current vectors of (a) OSCAR 15m current in time and space along the saildrone track, (b) saildrones 10-20 m current vectors averaged around each OSCAR ¼ degree data grid within 1 days to match OSCAR grids colored with saildrone 0.5 m salinity, and (c) their vector differences (saildrone - OSCAR) colored with saildrone 0.5 m temperature. OSCAR(1035), OSCAR(1036), and OSCAR(1037) are the corresponding OSCAR current in time and space along the saildrone track.

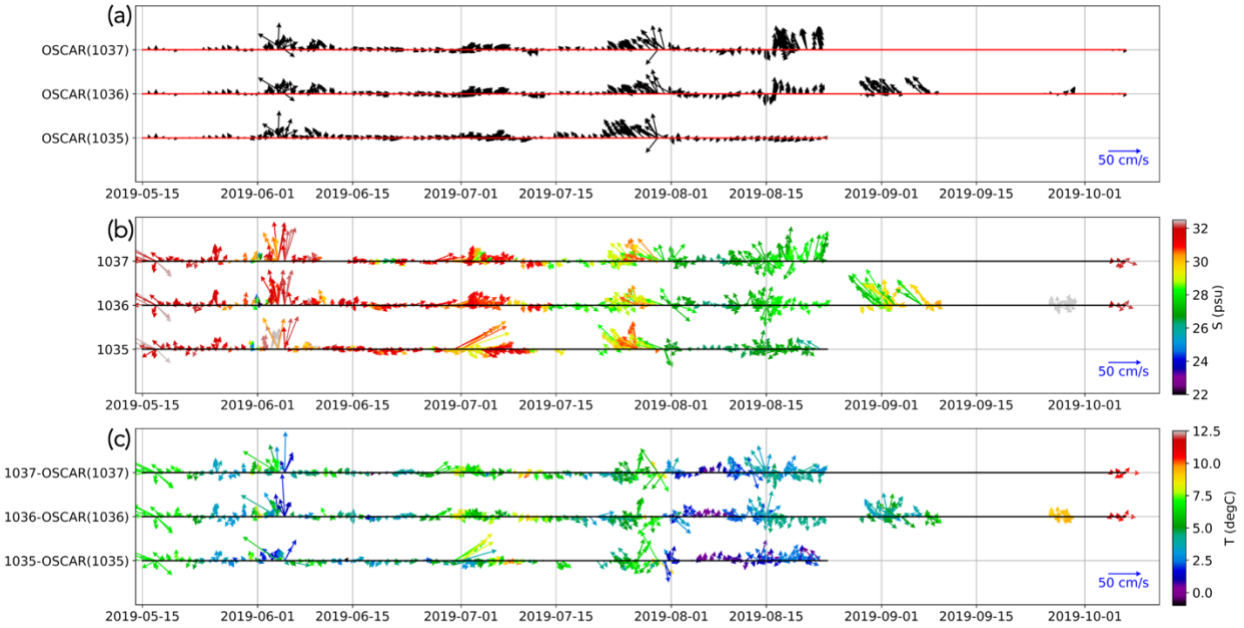

Figure 4: The wind rose plot summarizing the collocated vectors for (first column: a,e,i,m,q,u,y) saildrone 10-20 m averaged current vectors, (second column: b,f,j,n,r,v,z) OSCAR 15-m current vectors, (third column: c,g,k,o,s,w,aa) current speed difference (OSCAR - saildrone), and (last column: d,h,l,p,t,x,bb) vector correlation of the collocated pairs between OSCAR and saildrones. Each row represents the results of a specific subset of collocated vectors described in the subtitles on the left with the number of pairs in the parenthesis. The convention here is direction towards; i.e., the "spoke" towards "N" represents current flowing northward. The degrees in the rightmost column subplots (c,f,i,l,o,r,u) are the angle between the collocated OSCAR and saildrone current vectors. The values in the brackets for vector correlation colorbar are the limits of the cosine similarity. The unit of current speed is cm/s.

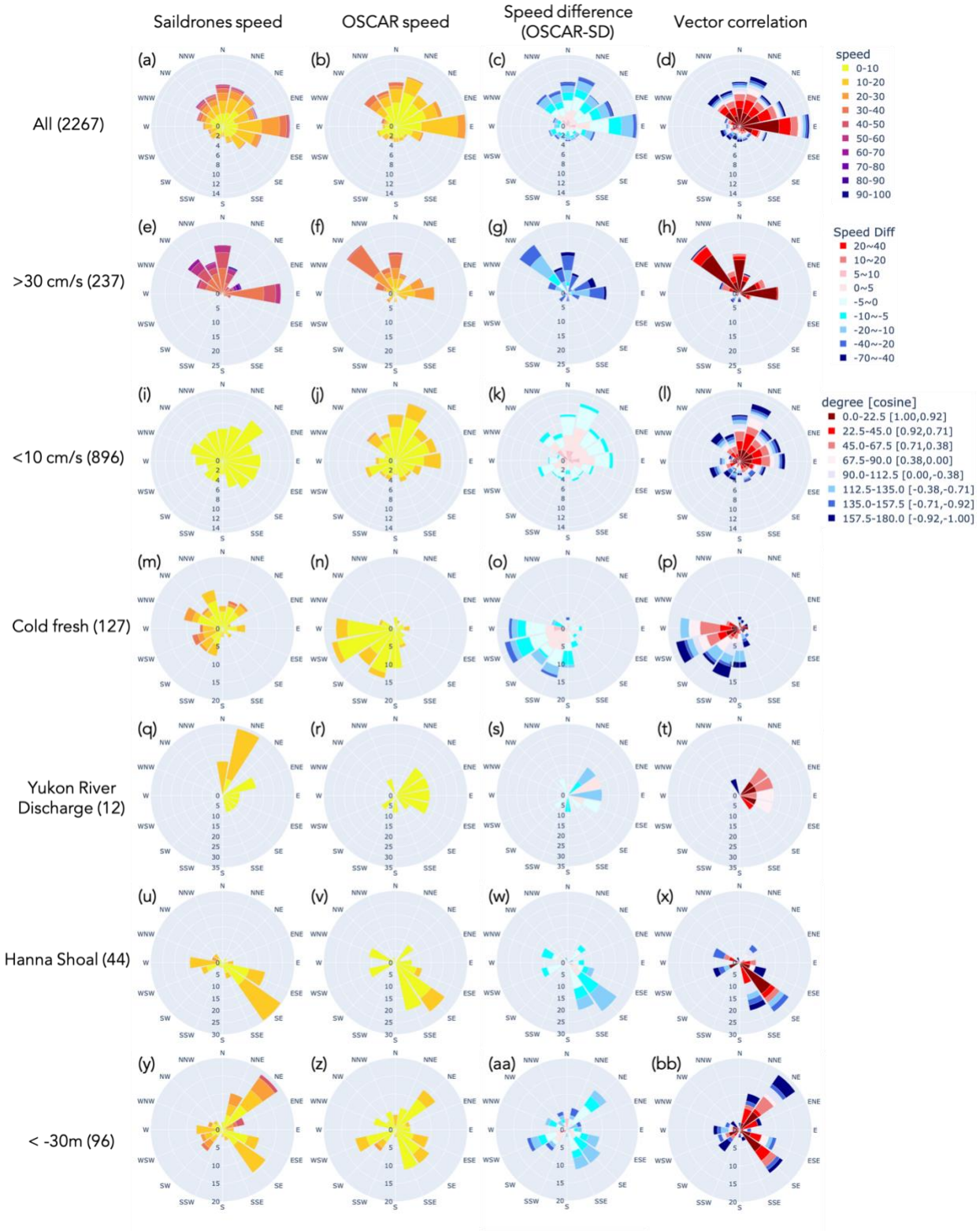
Saildrones speed
OSCAR speed
Speed difference (OSCAR-SD)
Vector correlation
All (2267)
>30 cm/s (237)
<10 cm/s (896)
Cold fresh (127)
Yukon River Discharge (12)
Hanna Shoal (44)
< -30m (96)
speed
0-10
10-20
20-30
30-40
40-50
50-60
60-70
70-80
80-90
90-100
Speed Diff
20~40
10~20
5~10
0~5
-5~0
-10~-5
-20~-10
-40~-20
-70~-40
degree [cosine]
0.0-22.5 [1.00,0.92]
22.5-45.0 [0.92,0.71]
45.0-67.5 [0.71,0.38]
67.5-90.0 [0.38,0.00]
90.0-112.5 [0.00,-0.38]
112.5-135.0 [-0.38,-0.71]
135.0-157.5 [-0.71,-0.92]
157.5-180.0 [-0.92,-1.00]

Figure 5: 2D histogram of (a) current speed (b) zonal current velocity and (c) meridional current velocity between the collocated saildrones and OSCAR data. The blue solid line is the linear regression line. The unit of the colors is the number.